eprints@whiterose.ac.uk
https://eprints.whiterose.ac.uk/

Granular Jamming Based Controllable Organ Design for Abdominal Palpation

Liang He[1], Nicolas Herzig[1], Simon de Lusignan[2], and Thrishantha Nanayakkara[1]

Abstract— **Medical manikins play an essential role in the training process of physicians. Currently, most available simulators for abdominal palpation training do not contain controllable organs for dynamic simulations. In this paper, we present a soft robotics controllable liver that can simulate various liver diseases and symptoms for effective and realistic palpation training. The tumors in the liver model are designed based on granular jamming with positive pressure, which converts the fluid-like impalpable particles to a solid-like tumor state by applying low positive pressure on the membrane. Through inflation, the tumor size, liver stiffness, and liver size can be controlled from normal liver state to various abnormalities including enlarged liver, cirrhotic liver, and multiple cancerous and malignant tumors. Mechanical tests have been conducted in the study to evaluate the liver design and the role of positive pressure granular jamming in tumor simulations.**

I. INTRODUCTION

Abdominal palpation is a technique widely used for primary diagnosis, where a general practitioner (GP) examines the patient's condition through direct haptic sensation [1]. During the procedure, physicians apply pressures on the patient's body with their palms and fingers to feel the size, form, position, texture, dullness, mobility, and tenderness of the organs. Palpation requires adequate hands-on experience and various techniques including controlling hand gesture, pressing position, speed, depth, force, and interaction with patients [1], [2], [3]. Currently, plastic manikins and real patients are used in palpation training for liver disease diagnosis and detection. However, plastic manikins can only give visual and geometry information, and the access to patients with a wide range of diseased conditions is limited. Useful medical simulators can significantly increase the learning efficiency of medical students and decrease the anxiety of the students in the training process[4]. A novel breast model for clinical breast examinations (CBEs) proposed by Gerling et al. shows that a dynamic model performs better than traditional models in training tactile palpation skills [5]. Inoue et al. developed an abdominal haptic device for palpation training through controlling two layers of flexible rubber sheets to simulate the stiffness changes of the human abdomen [6]. Hyde et al. created a human-like palpation prototype with pre-made replaceable liver models [7]. Researchers have also used pneumatic actuation for the simulation of shape and mechanical property of soft tissue [8], [9], [10]. Some other previous works of medical simulators focus on computer-aided virtual simulation, such as the virtual-reality index finger feedback simulator for prostate cancer diagnosis training designed by Burdea et al. [11] and the Virginia Prostate Examination Simulator [12]. These previous works explained the importance of the medical simulators in the training and education process. Accordingly, a dynamic controllable liver model that can give the students a practical sense of touch of diseased conditions has not yet proposed.

In this paper, we present a novel controllable liver design that can simulate various liver diseases by changing its size, stiffness, tumor numbers, and tumor sizes. The controllable organ design, shown in Fig. 1, is a pneumatic controlled silicone model with positive pressure granular jamming nodules and rubber balloon enlargement sections embedded. The design is capable of inflating one or more nodules from soft state to certain sizes of tumors. The granular jamming phenomenon within the membrane gives the nodule solid-like texture and "craggy" surface, which stimulate the malignant tumors. We will first describe the structure and design of the controllable organ in detail in section II. In section III, several indentation tests are presented to study the mechanical properties of the controllable organ and to prove the feasibility of the designed model. Finally, we conclude about the experiments and discuss the future development of the work in section IV.

L. He, N. Herzig and T. Nanayakkara are with the Dyson School of Design Engineering, Imperial College London, London, SW7 2AZ, UK l.he17@imperial.ac.uk, n.herzig@imperial.ac and t.nanayakkara@imperial.ac.uk

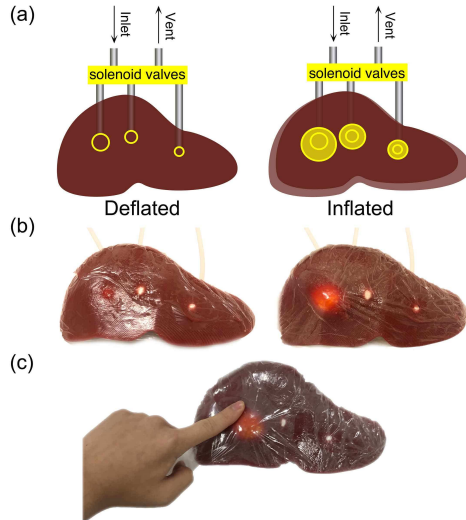[2]S. Lusignan is with Department of Health Care Management and Policy, University of Surrey, Guildford, UK s.lusignan@surrey.ac.uk

Fig. 1. (a) The liver design schematic diagram (b) Prototype with one left nodule inflated (c) Human palpation

II. CREATION OF THE CONTROLLABLE LIVER

A. Design Requirements

Several design requirements need to be carefully considered in the design of the controllable organ. Following requirements explain the main guideline for the design.

1) The purpose of the prototype is for clinical skills training. The model needs to be both realistic and easy to control for illustration.
2) The liver size and volume need to be designed based on clinical data; normal length of the liver span is 13.6 to 19 cm, height of the liver span is 6 to 12 cm, and weight is 1200 to 1500 g [2], [13].
3) The prototype needs to be modeled in three parts: tumor nodules, enlargement/stiffer section, and silicone liver body.
4) The material used for model making needs to have the stiffness similar to human liver to ensure realistic haptic sensation.
5) The surface of the model needs to be smooth. The liver is covered by peritoneum, a double-layered membrane that reduces the friction against other organs.
6) The model needs to be pneumatically controlled.
7) The liver needs to be able to stimulate the symptoms of various common liver diseases.
8) The control of the physical simulation of liver conditions needs to be stable.

B. Design Details

The liver model, shown in Fig. 1, is cast with a type of platinum-catalyzed silicone (Ecoflex, Smooth-On, Inc, USA) that has similar tactile property to human liver according to our mechanical test (discussed in the later section). The selected material is mixed with 1:1:2 ratio of Ecoflex 00:10 rubber part A, part B, and Smooth-On Slacker. Nodules and enlargement sections are embedded in the liver mold before the silicone is cured. Several pigments (Silc Pig, Smooth-On, Inc, USA) are added in the silicone to give the liver a realistic color for visual illustration. Granular jamming nodules are placed at the surface and bottom edge for surface tumor simulation and buried in the center of the liver to control the overall stiffness. Enlargement sections, which are made of only rubber balloon are buried at the back of the phantom to ensure liver enlargement with minimum stiffness change.

According to our previous research in the lab about granular jamming [14], we found that the granule size and membrane property determine the structural stiffness and the reverse process of it with positive pressure can be used for dynamic tumor simulation. The nodules, shown in Fig. 2, simulate the liver tumors with firm, inhomogeneous and craggy texture. The design has two layers of membranes with granules filled in between. The nodule shows an impalpable fluid-like state when deflated. With the inflation, the granules sandwiched by two membranes are continually compressed by the expansion of the internal membrane and starts transferring the granule layer to a solid-like structure. The area, stiffness, size, and hardness of the nodules can be therefore controlled by the pressure level of the granular jamming process.

C. Evaluation of Liver disease symptoms implemented in the prototype

The liver performs many functions in the human body from blood clotting, immunity, to protein and cholesterol production. On the other hand, as a critical organ that involves in many functions, many illnesses can affect the condition of the liver, such as Jaundice, cirrhosis, alcoholic liver disease, hepatitis, drug-induced hepatotoxicity, hepatocellular carcinoma, non-alcoholic fatty liver, liver tumors. Dynamic simulation of the pneumatic control is one of the biggest advantages of the design, which allows the model to present common diseases with customized liver conditions. With our prototype, we can simulate a variety of conditions of several liver diseases. Some common liver disease has been stated in Table I associated with palpation findings and model simulations.

TABLE I
ASSOCIATED LIVER DISEASES AND SIMULATIONS

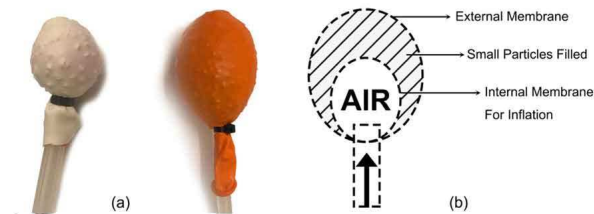| Liver disease	Condition by palpation	Relevant simulation model
Chronic hepatitis	Enlarged, firm texture, nodules rare	No nodules inflated, enlargement section inflated
Cirrhosis	Harder texture, may covered with hard nodules, enlarged	Surface nodules slightly inflated, enlargement section inflated
Hepatocellular carcinoma	Large and hard nodules	One or more nodules inflated
Malignant tumors	Large nodules	Several nodules inflated
Fatty liver	Enlarged	Enlargement section inflated

III. EXPERIMENTS AND TESTING

A. Material identification testing with porcine liver sample

A material study of several platinum-catalyzed silicone samples to identify the material that has the closest characteristics of the human liver has been performed. As it has been widely accepted, the porcine liver has a similar physical property of human liver. We used an ex-vivo porcine liver as a sample to identify the material for the liver model design. Five different samples have been made from Ecoflex 00-10

Fig. 2. (a) Granular jamming with positive pressure to simulate tumor (b) Schematic diagram
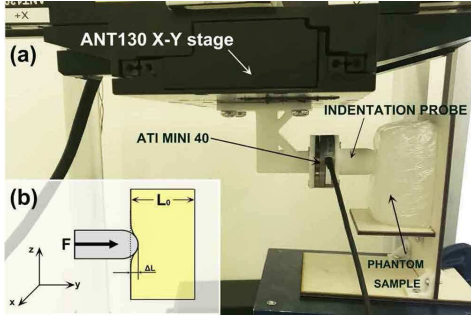
Fig. 3. (a) Experiment layout (b) Indentation diagram

(Smooth-on, USA), a versatile, safe and negligible shrinkage platinum-catalyzed silicone, and Slacker (Smooth-on, USA), a softener that can reduce material stiffness and make its property closer to human tissue. Sample A is pure Ecoflex 00-10 silicone with 90 g part A and 90 g part B. Sample B has the ratio of 1:1:1, with 60 g part A, 60 g part B, and 60 g Slacker. Sample C has the ratio of 1:1:2, with 45 g part A, 45 g part B, and 90 g Slacker. Sample D has the ratio of 1:1:3, with 36 g part A, 36 g part B, and 108 g Slacker. Sample E has the ratio of 1:1:4, with 30 g part A, 30 g part B, and 120 g Slacker. The dimensions of the five silicone samples are the same (around 7.5 mm x 7.5 mm x 3.5mm), the ex-vivo porcine liver has been cut to similar size. In this study, we compared the physical property of the five silicone samples with the ex-vivo porcine liver sample by applying a series of indentation tests. The experiment setup is shown in Fig. 3, with the 3D printed indentation probe (Length: 30 mm, Diameter: 20 mm) attaching on an ATI Mini40-E Force/Torque sensor (SI-40-2, ATI Industrial Automation, USA, resolution of 0.02 N) for data measurement. The probe structure is mounted on an ANT130 XY-stage (Aerotech Inc., accuracy of 2.5 μm) for the linear indentation movement. During the test, each phantom sample (including the ex-vivo porcine sample) have been probed from the indentation depth of 0.5 mm to 15.5 mm by step of 0.5 mm. Each indentation test has been repeated five times. The force data were collected during the test with LabView 2017 and National Instruments data acquisition cards PCIe-6320.

The ex-vivo porcine liver sample and five silicon samples show similar stress relaxation behavior during the test. Considering the complexity of the nonlinear viscoelastic property during the relaxation period, we compared the Young's Modulus after relaxation. The Young's modulus of each sample has been computed by linear regression of the stress by the strain. Thus the strain and the stress are computed from the force measured and the indentation as follows:

$$E = \frac{d\sigma}{d\epsilon} \tag{1}$$

$$\sigma = \frac{F_{relax}}{A(\Delta L)}, \tag{2}$$
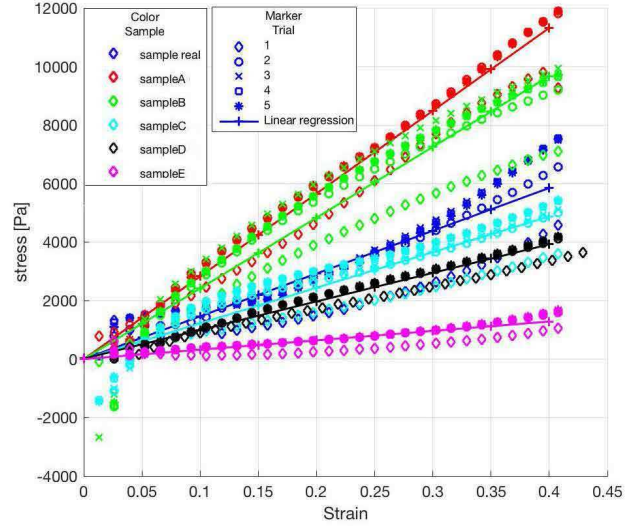
$$\epsilon = \frac{\Delta L}{L_0}. \tag{3}$$

Fig. 4. Young's modulus linear regression

where, E is the Young's modulus, σ is the stress, ϵ is the strain, F_{relax} is the compression force measurement after the relaxation, A is the contact area between the probe and the sample, L_0 is initial the thickness of the sample, ΔL is the indentation depth, see Fig. 3 (b). One can notice that due to the spherical shape of the end of the indentation probe, the contact area between the probe and the sample is dependent on the indentation. As shown in Fig. 4, the estimated Young's modulus of the samples, collected by computing the slope of the linear regressions, are 14.6 kPa for Porcine liver sample, 28.3 kPa for Sample A, 24.2 kPa for Sample B, 12.2 kPa for Sample C, 9.8 kPa for Sample D, and 3.2 kPa for Sample E. Sample C with the ratio of 1:1:2 of silicon part A, silicone part B and Slacker has the closest Young's modulus to the ex-vivo porcine liver among the five samples.

B. Granular jamming pressure/stiffness test

A set of pressure-stiffness tests have been conducted and discussed in this section to understand how different external membranes, granules (ground coffee), and different levels of pressure can attribute to the tumor simulation. Three different samples, shown in Fig. 5, have the same size internal balloons, 6.5×6.5 mm external PE membrane, and 9
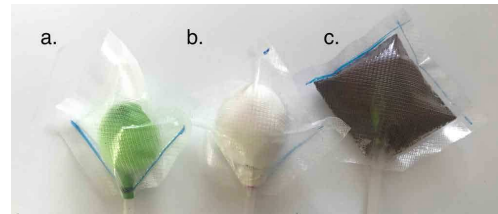

Fig. 5. (a) Sample 1, rubber membrane with external PE membrane, no ground coffee granules (b) Sample 2, double layered rubber membranes, ground coffee filled between two internal rubber layers, with external PE membrane (c) Sample 3, internal rubber membrane, ground coffee filled outside the rubber membrane, with external PE membrane
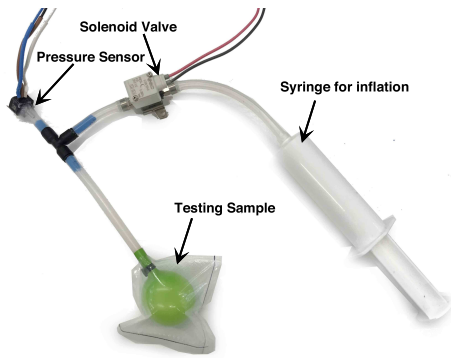
Fig. 6. Pressure/stiffness experiment set up

g ground coffee in samples 2 and 3. As shown in Fig. 6, the inflation was done manually with the syringe and the pressure data were collected before the start of each indentation test with a gauge pressure sensor (40PC250G2A, Honeywell). The solenoid valve (VDW10AA, SMC) was closed after the pressure reached each selected pressure level. The samples were then tested for three trials from 0.5 mm to 5 mm depth by steps of 0.5 mm with the experiment set up shown in Fig. 3. We observed linear property of the stiffness of the sample nodules and modeled it as a spring model $K = \frac{F}{X}$, where, K is the estimated stiffness value, F is the applied force, X is the displacement.

With computed linear regression of the mean value of the three trials, the stiffness of the samples for each selected pressure level has been estimated, as shown in Fig. 7. The external PE membrane limited the expansion of the nodules and kept the volume of the samples at a constant value in the experiment. Sample 1 and 3 reach the limit after the internal pressure increased to around 125 kPa. Sample 2 with the reverse granular jamming obtain high pressure (approximately 135 kPa) when it reaches the volume limit. Fig. 7 indicates that the three samples have similar property at high-pressure level. However, at the low-pressure level, the granules allow achieving high stiffness. The highest nodule stiffness is determined by the property of the external membrane, while granules can improve the stiffness at low-
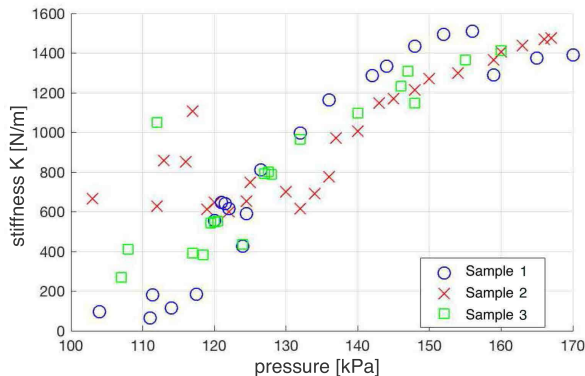
pressure level. Balloon expansion can expand the volume of the nodule with little change in stiffness.

IV. CONCLUSIONS

In this paper, we propose a novel design of dynamic controllable liver phantom for medical simulation through low positive pressure (< 120 kPa) granular jamming to create nodules with relatively high stiffness and realistic "craggy" surface texture for tumor simulation. The enlargement section of only rubber balloon allows the organ to be enlarged at low pressure with little stiffness change. The controllable liver model has been presented to a group of eight general practitioners in the UK to obtain feedback. Future work will focus on using this phantom to conduct human behavioral user studies of novices and experts.

ACKNOWLEDGMENT

Fig. 7. Stiffness-pressure curves for nodule types in Fig. 5

REFERENCES

[1] L. S. Bickley and P. G. Szilagyi, *Bates' Guide to Physical Examination and History Taking*, 12th ed. Philadelphia : Wolters Kluwer, 2017.

[2] C. Jarvis, *Physical examination & health assessment*, 7th ed. Elsevier B.V., 2015.

[3] S. Ramani, "Twelve tips for excellent physical examination teaching," *Medical Teacher*, vol. 30, no. 9-10, pp. 851–856, 2008.

[4] C. M. Pugh and L. H. Salud, "Fear of missing a lesion: use of simulated breast models to decrease student anxiety when learning clinical breast examinations," *American Journal of Surgery*, vol. 193, no. 6, pp. 766–770, 2007.

[5] G. J. Gerling, A. M. Weissman, G. W. Thomas, and E. L. Dove, "Effectiveness of a dynamic breast examination training model to improve clinical breast examination (CBE) skills," *Cancer Detection and Prevention*, vol. 27, no. 6, pp. 451–456, 2003.

[6] K. Inoue, K. Ujiie, and S. Lee, "Development of haptic devices using flexible sheets for virtual training of abdominal palpation," *Advanced Robotics*, vol. 28, no. 20, pp. 1331–1341, 2014.

[7] L. Hyde, C. Erolin, and J. Ker, "Creation of abdominal palpation model prototype for training of medical students in detection and diagnosis of liver disease," *Journal of Visual Communication in Medicine*, vol. 35, no. 3, pp. 104–114, 2012.

[8] A. Talhan and S. Jeon, "Pneumatic Actuation in Haptic-Enabled Medical Simulators: A Review," *IEEE Access*, vol. 6, no. March, pp. 3184–3200, 2017.

[9] A. A. Stanley, K. Hata, and A. M. Okamura, "Closed-loop shape control of a Haptic Jamming deformable surface," *Proceedings - IEEE International Conference on Robotics and Automation*, vol. 2016-June, pp. 2718–2724, 2016.

[10] N. Herzig, R. Moreau, A. Leleve, and M. T. Pham, "Stiffness control of pneumatic actuators to simulate human tissues behavior on medical haptic simulators," *IEEE/ASME International Conference on Advanced Intelligent Mechatronics, AIM*, vol. 2016-Septe, no. February, pp. 1591–1597, 2016.

[11] G. Burdea, G. Patounakis, V. Popescu, and R. E. Weiss, "Virtual reality training for the diagnosis of prostate cancer," *Ieee 1998 Virtual Reality Annual International Symposium, Proceedings*, vol. 46, no. 10, pp. 190–197, 1998.

[12] G. J. Gerling, S. Rigsbee, R. M. Childress, and M. L. Martin, "The design and evaluation of a computerized and physical simulator for training clinical prostate exams," *IEEE Transactions on Systems, Man, and Cybernetics Part A:Systems and Humans*, vol. 39, no. 2, pp. 388–403, 2009.

[13] D. C. Wolf, "Evaluation of the Size, Shape, and Consistency of the Liver," *Clinical Methods: The History, Physical, and Laboratory Examinations*, vol. 62, no. 6, pp. 478–481, 1990.

[14] A. Jiang, T. Ranzani, G. Gerboni, L. Lekstutyte, K. Althoefer, P. Dasgupta, and T. Nanayakkara, "Robotic Granular Jamming: Does the Membrane Matter?" *Soft Robotics*, vol. 1, no. 3, pp. 192–201, 2014.